

Mechanistic studies on percutaneous penetration enhancement by *N*-(4-halobenzoyl)-*S,S*-dimethyliminosulfuranes

D. J. Barrow, Jr.,* S. Chandrasekaran,* H. H. Heerklotz,[†] M. M. Henary,* B. B. Michniak,[§] P. M. Nguyen,* Y. Song,[§] J. C. Smith,^{1,*} and L. Strekowski*

Department of Chemistry,* Georgia State University, Atlanta, GA; Department of Biophysical Chemistry,[†] Biozentrum, University of Basel, Basel, Switzerland; and Department of Pharmacology and Physiology,[§] University of Medicine and Dentistry, New Jersey–New Jersey Medical School, Newark, NJ

Abstract Halogen-substituted iminosulfuranes are transdermal penetration enhancers (TPEs) in permeation studies using hairless mouse or human cadaver skin. The interaction of *N*-(4-*R*-benzoyl)-*S,S*-dimethyliminosulfuranes 1–4, where *R* = H, Cl, Br, and I, with 1- α -dimyristoyl-*sn*-glycero-3-phosphocholine (DMPC) has been studied using differential scanning calorimetry, isothermal titration calorimetry, nuclear Overhauser effect spectroscopy (NOESY), and NMR spectroscopy, and by calculation of the iminosulfurane polarizabilities in order to elucidate the molecular basis of the TPE activity. The active compounds reduce the melting temperature of the gel-to-liquid-crystal phase transition and induce multiple components in the transition excess heat capacity profile. The partitioning of the bromo derivative 3, the most active compound, into DMPC is unique in that 3 may be trapped in the bilayer, affording an enhanced residence time and a reason for its high TPE activity. The entropy decrease associated with the transfer of 3 to the bilayer is much lower than that for the other compounds, indicating that 3 occupies or induces sites that afford it considerable local motional freedom. Correlations between the iminosulfurane TPE activities, the partition coefficients, and NOESY cross-peak volume were observed. Molecular polarizabilities are not consistent with a TPE mode of action involving interaction of these agents with protein side chains.— Barrow, Jr., D. J., S. Chandrasekaran, H. H. Heerklotz, M. M. Henary, B. B. Michniak, P. M. Nguyen, Y. Song, J. C. Smith, and L. Strekowski. **Mechanistic studies on percutaneous penetration enhancement by *N*-(4-halobenzoyl)-*S,S*-dimethyliminosulfuranes.** *J. Lipid Res.* 2005. 46: 2192–2201.

Supplementary key words transdermal penetration enhancer • vesicle • bilayer • nuclear magnetic resonance • calorimetry • polarizability

The stratum corneum (SC) layer of the skin provides both protection from foreign substances and a barrier against dehydration. The protective properties of the SC, however, also inhibit most therapeutic agents from effectively

passing through the skin to their target when topically applied (1). The structure of the SC has been shown to consist of both hydrophilic and lipophilic regions. The lipophilic regions consist mainly of ceramides, cholesterol, and free fatty acids arranged in stacks of bilayers, which are thought to be responsible for the protective properties of the skin; it is this portion of the SC that must be breached in order to effectively deliver therapeutic agents transdermally (2–5). The mechanism of action of transdermal penetration enhancers (TPEs) is thought to be either through their intercalation into the lipid bilayers or through altering the solubility of the lipids. Comprehensive reviews of possible mechanisms have been published (1, 6).

Recently, there has been great interest in the development of agents that can facilitate the movement of substances across the skin barrier, in an attempt to increase the number of therapeutic agents that can be applied in topical preparations. A variety of classes of potential TPEs have been reported in the literature. Effective TPEs include sulfoxides, alcohols, fatty acids, and surfactants (6–8). One of the most investigated and effective TPEs to date is Azone[®] (Fig. 1). The interaction of Azone and other enhancers with the SC has been studied using a variety of techniques. The cohesiveness of the lamellae was disrupted by substances that were effective as a TPE, whereas the ineffective compounds did not disrupt the lamellae order (9–12).

We recently reported for the first time that iminosulfuranes 1–3 (Fig. 1) are potent TPEs (13, 14). This class of compound is isoelectronic with DMSO, a known TPE (1, 3, 4). Because halogeno-substituted iminosulfuranes 2 and 3 proved to be more potent TPEs than the parent com-

Abbreviations: CUP, cooperative unit parameter; DMPC, 1- α -dimyristoyl-*sn*-glycero-3-phosphocholine; DSC, differential scanning calorimetry; ER, enhancement ratio; FID, free induction decay; ITC, isothermal titration calorimetry; NOESY, nuclear Overhauser effect spectroscopy; SC, stratum corneum; T_m , melting temperature; TPE, transdermal penetration enhancer.

¹To whom correspondence should be addressed.
e-mail: chejcs@langate.gsu.edu

Manuscript received 1 April 2005 and in revised form 11 July 2005.

Published, JLR Papers in Press, August 1, 2005.
DOI 10.1194/jlr.M500123.JLR200

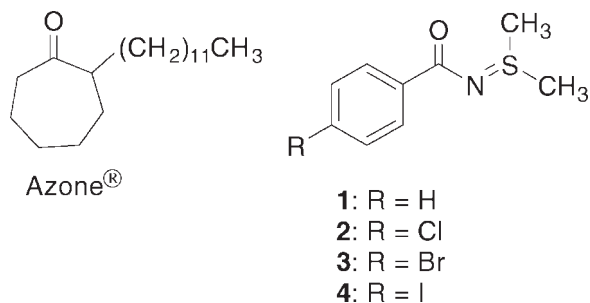


Fig. 1. Structures of Azone[®] and iminosulfuranes 1–4.

compound, 1, a new iodo derivative, 4, was synthesized as part of this work and tested in the previously used biological assay system. Values for enhancement ratio_J (ER_J) and Q₂₄ values for all compounds are contained in **Table 1**. ER_J is the ratio of the test drug (hydrocortisone) flux across skin samples in the presence of a selected iminosulfurane to the flux value observed in control experiments that contained no iminosulfurane (13, 14). Q₂₄ is the quantity of the test drug that passes through a unit area of the skin sample in 24 h. To obtain new information relevant to the mechanism of action of these TPEs, investigations have been performed to identify possible correlations of the biological effectiveness of 1–4 with their interaction with a well-defined model system consisting of lipid bilayers, as determined by isothermal titration calorimetry (ITC), differential scanning calorimetry (DSC), and proton nuclear magnetic resonance (¹H NMR). Azone was used as a reference TPE.

MATERIALS AND METHODS

General methods

Synthetic L- α -dimyristoyl-*sn*-glycero-3-phosphocholine (DMPC) was purchased from Avanti Polar Lipids (Alabaster, AL). The lipid was >99% pure. American Chemical Society-certified KCl, EDTA, and KH₂PO₄ were purchased from Fisher Scientific. HEPES was purchased from Sigma Chemical Co. (St. Louis, MO). Glass-distilled 99.9% D₂O was purchased from Isotec, Inc. (Miami-burg, OH). Azone was synthesized by using a published procedure (15–17).

TABLE 1. The transdermal penetration parameters ER_J and Q₂₄, calculated polarizabilities, and molecular volumes of the iminosulfuranes 1–4

| Compound | ER _J | Q ₂₄ μg/cm ² | Polarizability (Gaussian) | Polarizability (Thole) | Molecular Volume |
|----------|-----------------|---------------------------------------|------------------------------|---------------------------|---------------------|
| | | | | Å ³ | |
| 1 | 0.88 | 32.1 ± 10 | 147.9 | 126.1 | 227 |
| 2 | 1.51 | 61.9 ± 12.1 | 148.4 | 140.7 | 246 |
| 3 | 21 | 996 ± 192 | 155.5 | 148.5 | 252 |
| 4 | 1.6 | 121 ± 24 | — | 150.9 | 261 |

ER_J (enhancement ratio_J) is the ratio of the test drug hydrocortisone flux across skin samples in the presence of a selected iminosulfurane to the flux value observed in control experiments that contain no iminosulfurane (13, 14). Q₂₄ is the quantity of the model drug that passes through a unit area of the skin sample in 24 h.

Iminosulfuranes

The synthesis of 1–3 by the reaction of dimethyl(trifluoroacetoxy)sulfonium trifluoroacetate with the appropriate benzamide has been reported by us previously (13, 14). Iminosulfurane 4 was synthesized in a similar way from 4-iodobenzamide and crystallized from dichloromethane.

N-(4-iodobenzoyl)-*S,S*-dimethyliminosulfurane (4): yield 40%; mp 103–105°C; ¹H NMR (400 MHz, CDCl₃) δ 2.77 (s, 6H), 7.70 (d, J = 9.0 Hz, 2H), 7.81 (d, J = 9.0 Hz, 2H). Analysis: Calculated for C₉H₁₀INOS: C, 35.19; H, 3.28; N, 4.56. Found: C, 35.30; H, 3.35; N, 4.67.

Biological assay

The percutaneous penetration enhancement of 4 was assayed as described previously for 1–3 by using hydrocortisone as a model drug (13, 14). Toxicity studies on normal dermal fibroblasts and keratinocytes have been carried out using the 3-(4,5-dimethylthiazol-2-yl)-2,5-diphenyltetrazolium bromide (MTT) assay. At iminosulfurane concentrations of 0.1 and 0.2 M, no fibroblast cell death was noted; at 0.4 M iminosulfurane concentration, 60–84% cell viability was obtained, whereas at 0.8 and 1.2 M iminosulfurane concentrations, approximately 40% of the fibroblasts remained viable. Similar values were obtained when keratinocytes were employed in these assays (18). The iminosulfurane concentrations employed in the DSC, NMR, and ITC release protocols described herein did not exceed 1 mM.

Vesicle preparation

Small unilamellar vesicles were prepared according to a modification of the procedure of Suurkuusk et al. (19). This procedure produces unilamellar vesicles of nominally 300 Å diameter (20). For NMR work, the solid lipid was suspended in a D₂O medium consisting of 160 mM KCl and 10 mM KH₂PO₄ buffer, pH 7.4. For ITC work, DMPC was suspended in a 10 mM HEPES buffer, pH 7.4, with 160 mM KCl, and sonicated. For the DSC studies, large multilamellar vesicles were prepared by suspending DMPC in 10 mM HEPES buffer, pH 7.4, with 160 mM KCl. The suspension was stirred for 1 h, followed by 15 min of vortexing to yield a multilamellar preparation. The DMPC concentration was 10 mM for all experiments.

Differential scanning calorimetry

A portion of the liposome suspension was added to the iminosulfurane in solid form, and the suspension was stirred overnight at room temperature in order for the iminosulfurane to partition into the lipid bilayers. A control DSC scan was performed at 24, 48, and 72 h intervals on an aliquot of the liposome suspension without added ligand in order to check for possible changes in the excess heat capacity profile due to aging. No measurable changes were seen over the course of the experiment. Downscan data were collected by performing an upscan on an aliquot of DMPC containing 10 mol% iminosulfurane and then immediately performing a downscan on this sample. A second upscan and downscan were performed on the same preparation. This procedure was performed on a control consisting of an aliquot of a multilamellar DMPC preparation containing no iminosulfurane and was found to be completely reversible in all cases. DSC was performed with models DSC-VP and MC-2 instruments manufactured by Microcal, LLC (Northampton, MA).

Isothermal titration calorimetry

An aliquot of small unilamellar vesicles was added to the solid iminosulfuranes 1–4 so that the total iminosulfurane concentration was 10 mol%. This preparation was stirred overnight at 40°C. The preparation was then injected into HEPES buffer at 35°C, with an initial injection of 3 μl and subsequent injections of 10

μl , for a total of 30 injections. The release protocol described by Heerklotz, Binder, and Epanand (18) and Heerklotz and Seelig (19) was initially employed in determining partition coefficients. Isothermal titration binding studies were performed on instrument models MCS and VP-ITC manufactured by Microcal, LLC. Data were deconvoluted as described below using a release-and-incorporation algorithm running on Origin version 6.0 software by Microcal Software, Inc.

The partitioning of iminosulfuranes between buffer and bilayer is described by equation 1 (21, 22),

$$\phi = \frac{C_{D,b}}{C_D} = \frac{KC_L}{1 + KC_L} \quad (\text{Eq. 1})$$

where ϕ is the bound fraction of ligand, $C_{D,b}$ is the concentration of bound ligand, C_D is the total ligand concentration, C_L is the total lipid concentration, and K is the partition coefficient. As more of the lipid-ligand complex is injected into the buffer solution, there is a change in the degree of binding due to the accumulation of free drug. This change is described by equation 2.

$$\phi' = \frac{\partial\phi}{\partial C_L} = \frac{K}{(1 - KC_L)^2} \quad (\text{Eq. 2})$$

The normalized differential heat per mole, Q is described by equation 3,

$$Q = \frac{q}{V_0 \times \Delta C_L} = \quad (\text{Eq. 3})$$

$$[(C_D^{\text{int}} + R^{\text{SYR}} C_L) \times \phi'] + R^{\text{SYR}} (\phi - \phi^{\text{SYR}}) \Delta H_D^{f \rightarrow b} + Q_{\text{dil}}$$

where C_D^{int} (zero for the release protocol) is the amount of ligand in the cell initially, R^{SYR} is the mole ratio of ligand to lipid, ϕ^{SYR} is the bound fraction of ligand in the syringe, $\Delta H_D^{f \rightarrow b}$ is the enthalpy of the ligand going from the free to the bound form, and Q_{dil} is the heat of dilution. A nonlinear regression procedure was used to fit experimental data to a model defined by Heerklotz, Binder, and Epanand (21) using equations 1–3.

Nuclear magnetic resonance

An aliquot of small unilamellar vesicles was added to the solid ligand so that total iminosulfurane concentration was 10 mol% or 1 mol%. This preparation was stirred overnight at 40°C, followed by nuclear Overhauser effect spectroscopy (NOESY) studies carried out at 35°C using a Unity 600 spectrometer manufactured by Varian Associates, Inc. (Palo Alto, CA), using the TN NOESY pulse sequence with a 0.1 s mixing time; 2,048 data points were collected over 256 increments with 96 acquisitions, using a 5,092 Hz spectral width. Data analysis was carried out using the Varian software package VNMR (23). A 60°-shifted sinebell window function was employed in both dimensions, and zero filling was carried out in the F1 and F2 dimensions. The first two data points in the free induction decay (FID) were determined using linear prediction based on the first 50 points in the FID with $\text{lpfit} = 16$ (24). Baseline correction in both dimensions was employed via a fourth-order polynomial using the procedure of Brown (25).

Polarizability calculations

Two types of polarizability calculations were performed. Molecular orbital calculations were performed using the Gaussian 98 software package at the Hartree-Fock level. The basis set employed was UHF/6-31+g(2d,3pd) (26). A geometry-optimized structure for each iminosulfurane on which polarizability calculations were performed was obtained from ab initio calculations using a 3-21* basis set. Two separate calculations were performed on each iminosulfurane, with the exception of 4, which requires

relativistic corrections not included in the basis set described above. One calculation was performed with the dielectric constant of unity, and one was performed with the dielectric constant of 1.92 in order to simulate a hydrophobic environment. Similar results were obtained from these two calculations. The second type of polarizability calculation employed the Thole model, which sums the atomic polarizabilities. This model was applied to the same geometry-optimized iminosulfurane structures used in the molecular orbital theory calculations. The induced dipole at point p (μ_p) is given by equation 4,

$$\mu_p = \alpha_p \left[F_p - \sum_{p \neq q}^N T_{pq} \mu_q \right] \quad (\text{Eq. 4})$$

where α_p is the atomic polarizability tensor at p , F is the homogeneous electric field, T_{pq} is the dipole field tensor, and μ_q is the induced dipole at point q . These calculations were performed using the POLAR algorithm provided by Van Duijnen and Swart (27). Molecular volumes of the iminosulfuranes were calculated using molecular mechanics via the PCMODEL computational package.

RESULTS

Biological activity

The biological activities of iminosulfuranes 1–4 are collected in Table 1 in terms of the flux ER_j and the Q_{24} . Compound 1 ($R = \text{H}$) has a low Q_{24} value and an ER_j value of less than unity, indicating that it actually increases the skin barrier relative to the control. Compounds 2 and 4 have comparable ER_j values, but the iodo derivative 4 exhibits a larger Q_{24} value relative to that of compound 2. Compound 3 ($R = \text{Br}$) is the most active agent of this series. The ER_j value of compound 3 exceeds that of the other iminosulfuranes by over an order of magnitude, with a correspondingly large Q_{24} value.

Differential scanning calorimetric studies

All compounds investigated using DSC, with the exception of Azone, attenuate within 4 h the pretransition signal amplitude shown in the control DMPC DSC scan (Fig. 2). The pretransition is nearly broadened into the baseline by all compounds studied, and the residual amplitude remains constant over time. Because the pretransition is thought to be caused by the reorientation of the lipid headgroups, any compounds that approach the headgroup region of the bilayer could perturb the pretransition. The data collected are consistent with all iminosulfuranes approaching the headgroup region of the bilayer. The constant pretransition residual amplitude also implies that transfer of the iminosulfuranes to the bilayer is complete on a time scale of 4 h.

The gel-to-liquid-crystal phase transition of DMPC is affected differently by compounds 1–4. Compound 3, which exhibits the strongest activity as a TPE, also causes a shoulder to appear at a temperature below the main phase transition of DMPC. The data could not be simulated using a single two-state model, but can be accurately simulated using a sum of two or more two-state models. The multiple two-state model suggests that 3 destabilizes the bilayer, as

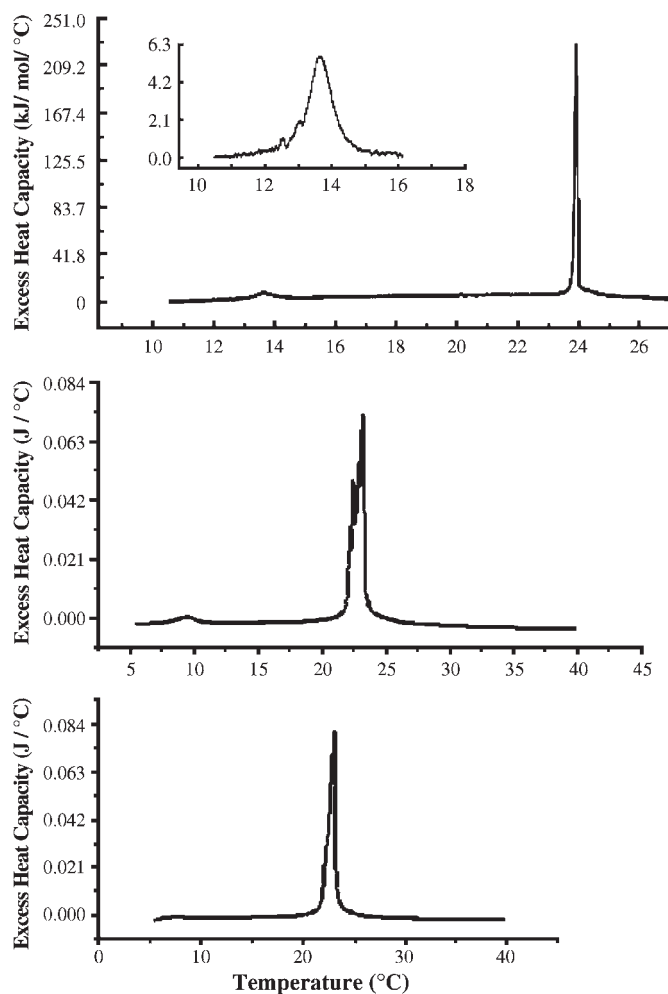


Fig. 2. The excess heat capacity profiles of L- α -dimyristoyl-*sn*-glycero-3-phosphocholine (DMPC) phase transitions; the inset is the pretransition at 14°C (top panel). A downscan of DMPC with 10 mol% compound 3 present: after 24 h (middle panel) and after 72 h (bottom panel).

manifested by a reduction in the phase transition temperature (T_m). When the sum of three two-state transitions is used (**Fig. 3**) to simulate the phase transition, there is improved agreement with collected data, especially at the 72 h exposure interval. This observation suggests the formation of multiple melting domains within the bilayer. A downscan (decreasing temperature) was performed on the DMPC-2, DMPC-3 and DMPC-4 preparations. The downscans of DMPC-2 and DMPC-4 are completely reversible, as observed in subsequent upscans at 24 h, 48 h, and 72 h. The downscans of DMPC-3 are reversible at 24 h and 48 h but not at 72 h (**Fig. 4**). The 24 h upscan is bifurcated, with one peak on the leading shoulder of the excess heat capacity profile and closer to the melting temperature (T_m) of pure DMPC. When the downscan was performed, the analogous first peak was no longer present. Additional upscans on the same preparation were no longer bifurcated. The excess heat capacity profiles of DMPC containing 4 and DMPC containing 2 are similar to that of DMPC containing 3 (data not shown). However, 2 and 4

seem less adept at the formation of multiple melting domains in the bilayer, based on the fact that a dual two-state model adequately describes the DMPC excess heat capacity profile data at the 72 h time interval. The excess heat capacity profile of the gel-to-liquid-crystal phase transition of DMPC containing 1 shows no differences when compared with that of the DMPC phase transition without added ligand, with the exception of the attenuation of the pretransition (data not shown).

Studies were performed at 1 mol% on the compounds that perturbed the gel-to-liquid-crystal phase transition at 10 mol%. The excess heat capacity profile of DMPC with 1 mol% 2 was indistinguishable from that of the DMPC control (data not shown), and the excess heat capacity profile of DMPC preparations containing 1 mol% 3 or 4 could be described as a single two-state system (see **Fig. 4** for 3; data not shown for 4). However, the cooperativity of the gel-to-liquid-crystal transition was lowered with the addition of either 1 mol% 3 or 1 mol% 4 (*vida intra*).

The excess heat capacity profile of DMPC with 1 mol% 3 has subtle differences from the excess heat capacity profile of DMPC alone. The enthalpy of the phase transition remained constant over time at 23.0 ± 1.2 kJ/mol, and the T_m remained constant at $23.9 \pm 0.02^\circ\text{C}$. In the case of 4, the enthalpy change remained invariant with time at 20.5 ± 1.7 kJ/mol, and the T_m remained constant at $23.7 \pm 0.03^\circ\text{C}$. In order to further explore any potential perturbation of the DMPC bilayer upon addition of 1 mol% 3, the cooperative nature of the transition was explored. The cooperative unit parameter (CUP) is defined by equation 5,

$$\text{CUP} \equiv \frac{\Delta H_{VH}}{\Delta H_{cal}} \quad (\text{Eq. 5})$$

where ΔH_{VH} is the van't Hoff or apparent enthalpy defined by equation 6. Note that the CUP is meaningful for two-state systems only.

$$\Delta H_{VH} = \frac{4RT_m^2 \Delta C_{p_{max}}}{\Delta H_{cal}} \quad (\text{Eq. 6})$$

For a two-state system, i.e., gel-to-liquid-crystal transition or folded-protein-to-unfolded-protein transition, the CUP is unity or greater. The higher the CUP, the larger the cluster size that melts as a single unit. The addition of 1 mol% 3 to DMPC results in a 35% reduction in the CUP within the first 24 h of addition, relative to that for the control DMPC, with no statistically significant change in the CUP over the next 48 h. The addition of 1 mol% 4 to DMPC causes a 48% reduction in CUP within the initial 24 h after addition to the lipid preparation, with no statistically significant change in the CUP observable over the next 48 h. Results are summarized in **Table 2** (28–30). Note that the observation of constant ΔH , T_m , and CUP values in these experiments suggests that equilibrium has been established with the bilayer in less than 24 h.

When Azone was added to DMPC large multilamellar vesicles at 10 mol% concentration and under the previously stated conditions, there was no detectable perturbation of the phase transition excess heat capacity profile

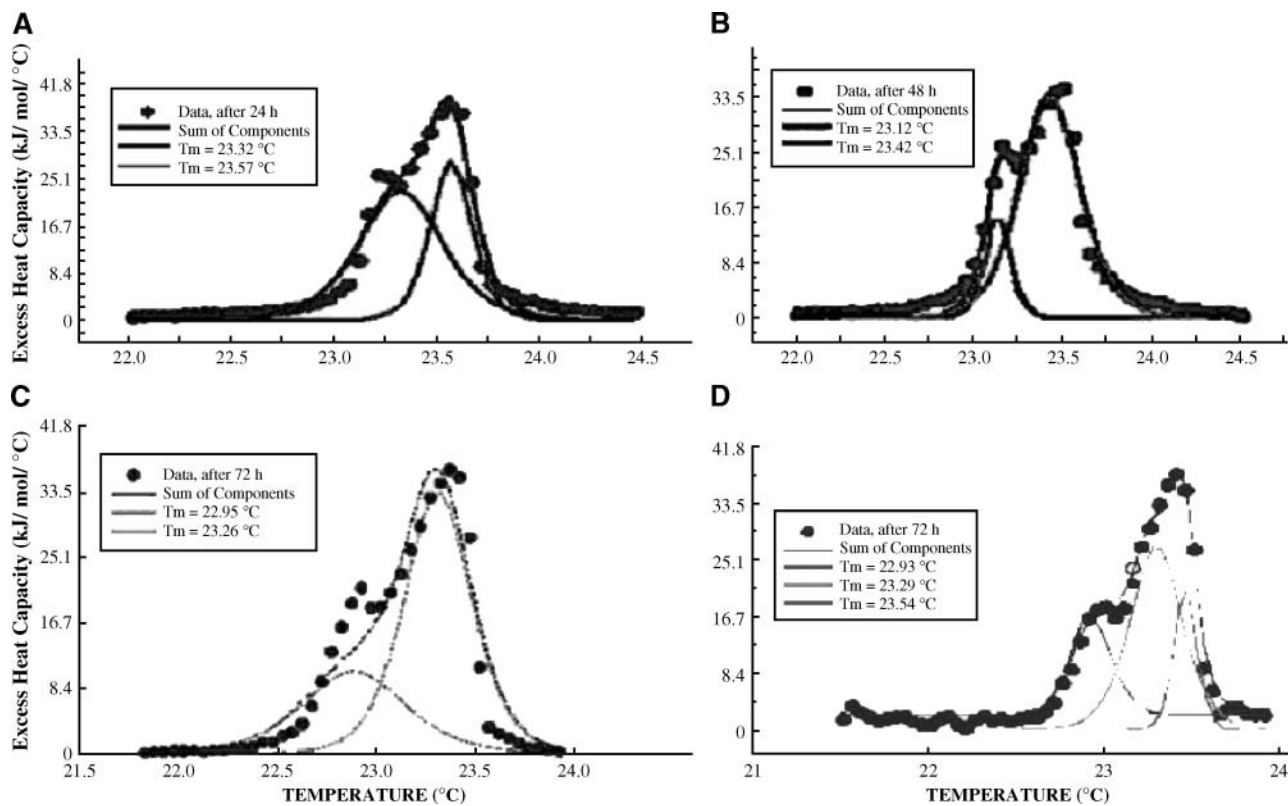


Fig. 3. The excess heat capacity profile of 1- α -dimyristoyl-*sn*-glycero-3-phosphocholine (DMPC) with 10 mol% of compound 3 added. A: After 24 h fit to a two-component model. B: After 48 h fit to a two-component model. C: After 72 h fit to a two-component model. D: After 72 h fit to a three-component model.

within 72 h. The phase transition data for the DMPC-Azone system could be described as a single two-state model, and the pretransition was observable in the excess heat capacity profile (data not shown). The ΔH and T_m values of this system are not statistically different from those of the control DMPC preparations. The CUP parameter (which is very sensitive to the presence of ligands) for this system is also not statistically distinguishable from that of the DMPC control. These observations are in direct contrast to those reported by Rolland et al. (31, 32) for a preparation using DMPC that had been dissolved with Azone in

chloroform, the chloroform then removed, and the DMPC-Azone film that remained resuspended in buffer. These observations suggest that Azone may not transfer to the DMPC preparation in any appreciable quantity on the time scale of these experiments.

Nuclear magnetic resonance studies

Strong crosspeaks from the interaction of the phenyl protons of both 3 and 4 with the fatty acid methylene and choline *N*-methyl protons of DMPC are observed in the NOESY spectra. In addition, the spectrum of 3 exhibits a

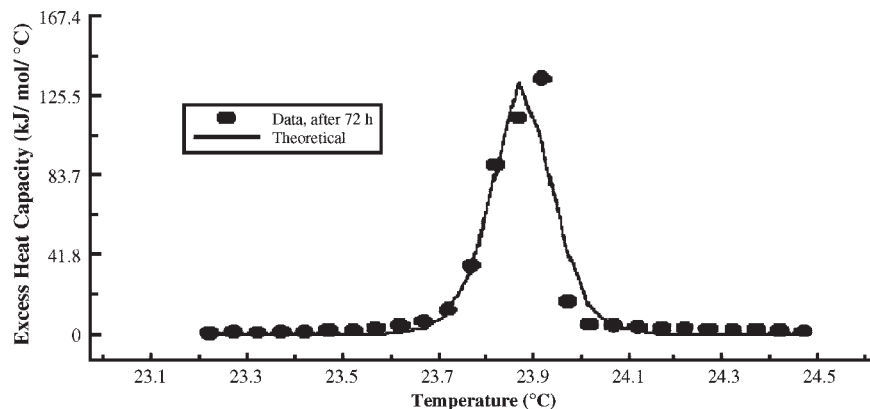


Fig. 4. The excess heat capacity profile of DMPC with 1 mol% compound 3 added after 72 h. The data are described by a single two-state model.

TABLE 2. The effect of compounds 3 and 4 present in DMPC multilamellar preparations at 1 mol% on the CUP computed using equation 5

| | Average CUP | Standard Deviation |
|------|-------------|--------------------|
| DMPC | 1122 | 53.33 |
| 3 | | |
| 24 h | 718.4 | 29.83 |
| 48 h | 722.5 | 49.36 |
| 72 h | 750.2 | 85.30 |
| 4 | | |
| 24 h | 585.4 | 83.37 |
| 48 h | 579.5 | 98.40 |
| 72 h | 632.7 | 132.1 |

CUP, cooperative unit parameter.

crosspeak to the terminal methyl protons of DMPC that is not observed in the NOESY spectrum obtained for the DMPC-4 preparation (Fig. 5). Crosspeak volume values for the unresolved fatty acid methylene protons to the aromatic protons of the iminosulfuranes are 2.10, 9.08, and 5.79 mm³ for compounds 2, 3, and 4, respectively. Crosspeaks from the phenyl protons of 2 to the DMPC protons are much weaker than those observed in the DMPC-3 spectrum, suggesting less extensive penetration into the bilayer; no crosspeaks to the terminal methyl or choline *N*-methyl protons are observed under the same analysis conditions used in the DMPC-3 spectrum. There are no detectable crosspeaks in the spectrum of DMPC-1 with 10 mol% iminosulfurane or in the spectrum of DMPC-3 or DMPC-4 with 1 mol% iminosulfurane present.

There is no evidence to suggest that the iminosulfuranes are causing vesicle fusion, based on visual inspection of these preparations and the lack of iminosulfurane-induced broadening of the proton NMR lines, especially those associated with protons in the glycerol backbone region that have limited motional freedom, the line widths of which should reflect the overall vesicle tumbling process.

Isothermal titration calorimetry

The isotherm for DMPC containing 10 mol% 3 (Fig. 6) has a large heat evolved from the initial injection, with heats becoming smaller with each successive injection until the heats evolved become constant. The data were deconvoluted assuming that the bilayer was permeable to the ligand on the timescale of the ITC experiment. The results are tabulated in Table 3. The directly measured ΔH values were significantly different when the release and the incorporation procedures were employed. This observation suggests that a portion of bilayer-associated 3 may be unable to leave the inner leaflet on the time scale of the experiments, based on the release protocol. The data for compound 3 were then deconvoluted using a model based on an impermeable bilayer. This model led to virtually the same values for ΔH and K when the release and incorporation protocol data were analyzed. Results from this analysis are shown in Table 4, where the values of the δ parameter indicate the fraction of accessible ligand (δ_D) and accessible lipid (δ_L). For fully accessible sites, δ values are unity, and for the case in which only the outer leaflet

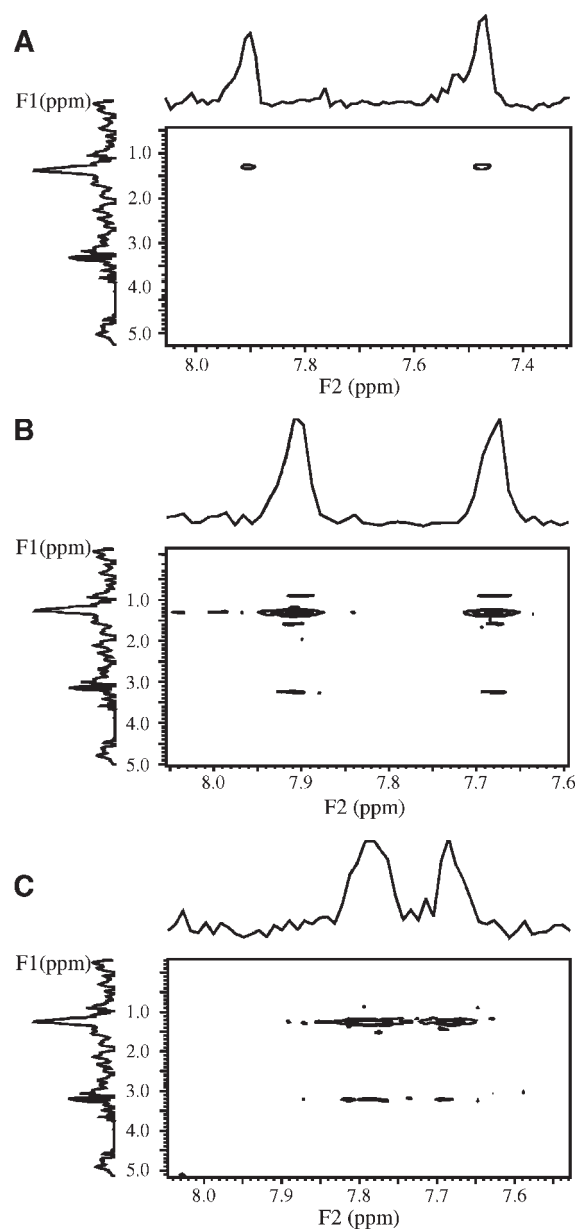


Fig. 5. Nuclear Overhauser effect spectroscopy (NOESY) spectra of DMPC vesicles: with 10 mol% of compound 2 added (A), with 10 mol% of compound 3 added (B), and with 10 mol% of compound 4 added (C). Crosspeaks at 0.8, 1.2, and 3.3 ppm on the vertical axis correspond to the DMPC terminal methyl, unresolved fatty acid methylene, and the choline *N*-methyl protons, respectively. The two projections on the top horizontal axis are resonances due to the two sets of phenyl protons.

of the bilayer is accessible, δ is 0.6. The isotherms for DMPC-1, DMPC-2, DMPC-4 and DMPC-Azone preparations all at 10 mol% ligand were also deconvoluted, with δ being unity. The ΔH values obtained from the incorporation and release protocols are in agreement (Table 3) for compounds 2 and 4. No detectable binding of compound 1 or Azone to DMPC vesicles was observed.

Polarizability calculations

Using the Thole model and molecular orbital (MO) calculations, the polarizabilities of each of the iminosul-

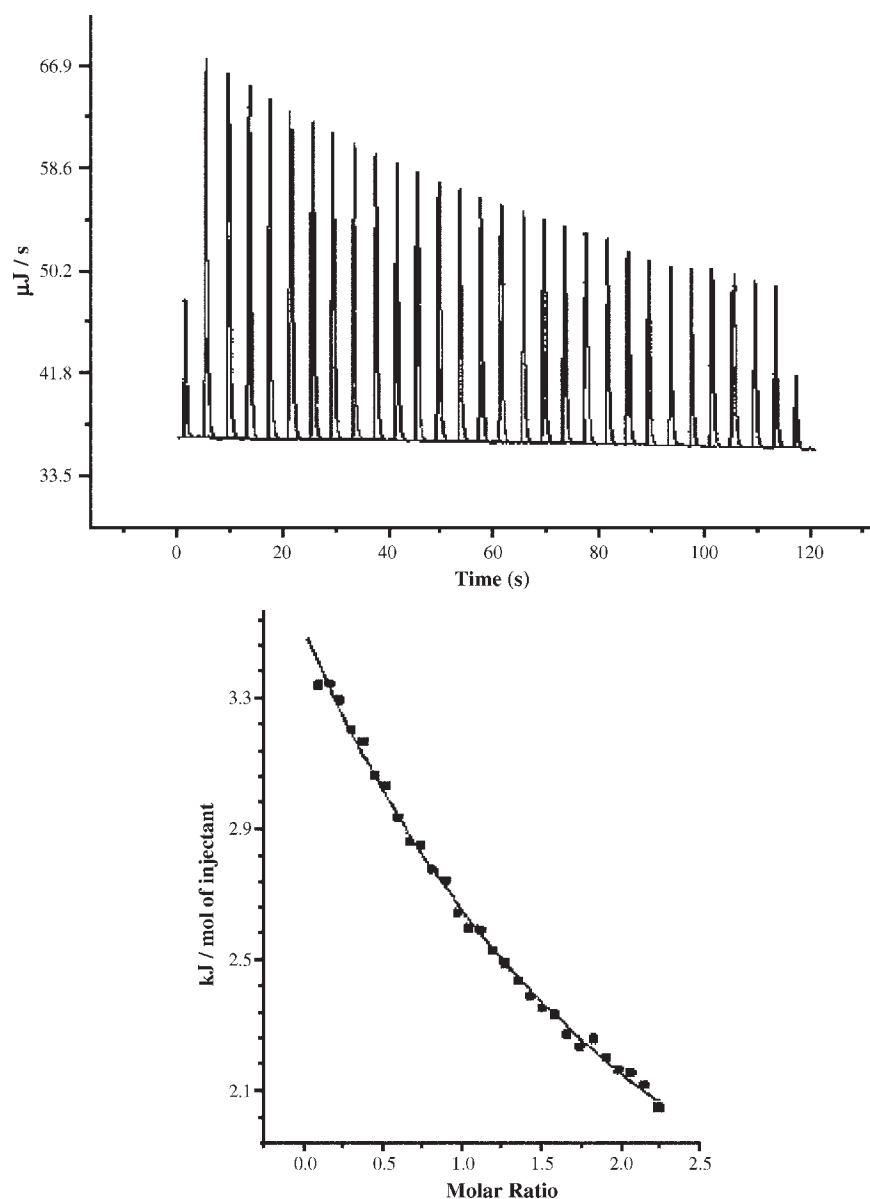


Fig. 6. Release isotherm of DMPC-3 complex performed at 35°C. Raw data (top) and theoretical fit (bottom) to data (square plotting symbols).

furans 1–4 were calculated. The results for a dielectric constant of unity are collected in Table 1 and are reported in volume units. The polarizability values reported from MO calculations are the average of the tensor trace. There is an increase in the polarizability as the effectiveness of

the TPE increases, with the exception of 4; the polarizability values do not attain a maximum for the most active compound, 3.

DISCUSSION

Partition coefficient data determined using ITC indicate that the iminosulfurane with the largest partition coefficient induces the largest flux of the test drug hydrocortisone (J) across skin preparations. Compounds 3 and 4 cause the greatest perturbation to the gel-to-liquid-crystal phase transition of DMPC; both of these compounds also lower the T_m and induce multiple domains. This perturbation of the gel-to-liquid-crystal phase transition correlates with J.

TABLE 3. Parameters obtained from isotherms of compounds 2–4 based on a permeable bilayer model ($\delta = 1$)

| Compound | Release Protocol | Incorporation Protocol |
|----------|---------------------|------------------------|
| 2 | K (1/mM) | 0.028 ± 0.021 |
| 2 | ΔH (kJ/mol) | -26.6 ± 0.8 |
| 3 | K (1/mM) | 0.26 ± 0.02 |
| 3 | ΔH (kJ/mol) | -2.59 ± 0.15 |
| 4 | K (1/mM) | 0.066 ± 0.01 |
| 4 | ΔH (kJ/mol) | -38.3 ± 0.5 |

TABLE 4. Parameters obtained from isotherms of compound 3 assuming a permeable bilayer ($\delta = 1$) or an impermeable bilayer ($\delta = 0.6$) model

| | Release | Incorporation |
|---------------------------------|------------------|------------------|
| δ_1 and $\delta_D = 1.0$ | | |
| K (1/mM) | 0.26 ± 0.02 | 0.68 ± 0.04 |
| ΔH (kJ/mol) | -2.59 ± 0.15 | -3.85 ± 0.14 |
| $\delta_1 = 0.6$ | | |
| K (1/mM) | | 0.61 ± 0.08 |
| ΔH (kJ/mol) | | -4.26 ± 0.15 |
| δ_1 and $\delta_D = 0.6$ | | |
| K (1/mM) | 0.43 ± 0.07 | |
| ΔH (kJ/mol) | -4.32 ± 0.13 | |

The properties and effects of 3 on a DMPC bilayer differ from those of the other iminosulfuranes that have been investigated. The partition coefficient obtained using the incorporation protocol is significantly larger than that obtained using the release protocol if the permeable bilayer model ($\delta = 1$) is employed. In addition, the DMPC-3 excess heat capacity profile is also altered after the sample is heated, whereas the excess heat capacity profile of all other iminosulfuranes studied does not change. The initial upscan performed contains a bifurcated peak that is consistent with the presence of two thermodynamically distinct regions in the bilayer, each region containing a set of sites with differential local concentrations of 3. Previous studies utilizing cholesterol have suggested such a distribution (33). These observations suggest that a barrier exists which prevents the uniform distribution of 3 throughout the bilayer. Upon heating and scanning down in temperature, the bifurcation is no longer seen, and the absence of the bifurcation remains on any further upscans performed on the preparation. This observation suggests that upon heating, 3 undergoes a uniform distribution and that cooling the bilayer does not affect the redistribution. Below the transition temperature, the acyl chains of the bilayer are in an ordered, rigid gel state, but after the transition, there is more movement of the acyl chains and less resistance to diffusion in the acyl region of the bilayer, which would facilitate uniform distribution of 3 in the DMPC preparation.

The existence of a distribution barrier or kinetic trap is also suggested by the difference in the partition coefficient derived from the incorporation experiment versus the release experiment. That the partition coefficient determined by the incorporation protocol exceeds that obtained using the release protocol when the data are analyzed using the fully permeable bilayer model, $\delta = 1$, may reflect the enhanced availability of binding sites in the bilayer outer leaflet associated with the incorporation methodology in which a fixed quantity of iminosulfurane is titrated with DMPC vesicles. The observation of a crosspeak between the phenyl protons of compound 3 and those of the terminal methyl group of the DMPC acyl chain, however, suggests that a least a portion of the bound fraction of this compound is penetrating substantially into the bilayer under extended periods of exposure of the bilayer to compound 3. The dynamics of DMPC lipids, however, in-

clude a mode in which some of the acyl chains reach the surface of the bilayer, as manifested by a crosspeak between the choline $N(\text{CH}_3)_3$ protons and those of the acyl chain terminal methyl group. The crosspeak associated with this interaction is observed in the NOESY spectra collected for these investigations but is much smaller than that associated with other lipid-lipid NOE interactions. A model in which this mode of motion of the DMPC acyl chains is viewed as the dominant one would uniquely restrict the interaction of compound 3 to outer leaflet sites at or near the bilayer surface, i.e., 3 would not penetrate the DMPC bilayer on the time scale of these experiments.

The cross polarization transfer rate associated with the aforementioned interaction mode is, however, approximately an order of magnitude smaller than that characterizing interaction between the acyl terminal methyl group protons and those of DMPC moieties near this group (34). An additional observation also argues against this mode of interaction as the prime source of the aforementioned NOESY crosspeak. Compounds 3 and 4 have substantial surface populations at very similar sites, as indicated by the strong crosspeaks between the phenyl protons of these compounds and those of the choline N -methyl groups, but the crosspeak to the acyl terminal methyl group is only observed for compound 3. This observation argues for a differential depth of penetration characterizing the interaction of these compounds with the DMPC bilayer, with compound 3 occupying sites that are located deeper in the bilayer than are those occupied by compound 4. Such a deep penetration is consistent with an overnight exposure period of the bilayer prior to the initiation of NOESY data collection that extended for 72 h thereafter. The binding studies further suggest that once occupied, a subset of sites, which may reside at least in part on the inner leaflet due to the putative enhanced permeation and disordering of the bilayer by 3, does not release compound 3 on the time scale of the release ITC protocol. Such a location and slow release from the bilayer would favor an enhanced bilayer residence time for compound 3 in comparison to that of the other compounds in this series and, if also present in the skin preparations used for pharmacological studies reported herein, may afford an explanation, at least in part, for the markedly larger activity of compound 3 in comparison to the other compounds utilized in these investigations.

NOESY spectra are consistent with the strongest binding of 3 to the bilayer, and with the distribution of both 3 and 4 into various parts of the DMPC bilayer that is also consistent with the multicomponent gel-to-liquid-crystal phase transition excess heat capacity profiles. There is a correlation between methylene crosspeak volume and the flux, J , and Q_{24} . However, NOESY crosspeak volumes are dependent not only on population but also on inter-proton distance between the aromatic protons of the iminosulfuranes and the protons of the several DMPC moieties. This analysis further assumes that the respective crosspeak buildup rates are the same for each of the iminosulfuranes investigated.

The calculated polarizabilities and molecular volumes

of iminosulfuranes 1–4 correlate poorly with the biological activity of these compounds (Table 1). Polarizability is thought to provide an important contribution to the activity of compounds, the mechanism of action of which is via interaction with the aromatic amino acid units of proteins (1). The polarizability and molecular volume results are not consistent with the interaction of the iminosulfuranes with proteins.


Because the partition coefficients, K , and the ΔH for ligand partitioning into DMPC preparations were obtained experimentally, it was possible to obtain the entropy change associated with the partitioning of the iminosulfurane compounds into the bilayer.

(Table 5). The ΔS values are negative for all iminosulfuranes studied and indicate the expected loss of rotational and translational freedom of the ligands when they associate with the small DMPC vesicles in which the acyl chains are more disordered than is the case with larger vesicles. Hence, compensation for the entropy loss on binding to small vesicles due to additional disordering of the acyl chains by the iminosulfuranes is minimal (35). In the case of 3, however, the absolute magnitude of the ΔS value is nearly an order of magnitude lower than that of the other iminosulfuranes. This result suggests that there is a considerable compensation for the loss in entropy upon binding of compound 3 to the DMPC preparations and further suggests that 3 has access to regions of the bilayer that afford it considerable local motional freedom and/or that bound 3 induces regions in which it and DMPC lipids have enhanced motional freedom. An additional compensating entropy effect may arise from the release of bound water from apolar surfaces due to the disruptive activity of 3. These observations are consistent with a mode of action of compound 3 in which disruption of the DMPC bilayer originates from surface binding sites of this compound, perhaps followed by substantial penetration of this compound into the bilayer. In initial binding studies, it was observed that a fixed quantity of DMPC vesicles, when titrated with compound 3, could not be saturated with this ligand and appeared to bind it without limit, with probable considerable disruption of the bilayer structure. These observations are consistent with the large perturbation of the gel-to-liquid-crystal phase transition excess heat capacity profiles observed in DSC work on the DMPC-3 system and correlate with the high activity of 3 in the pharmacological studies using human cadaver or hairless mouse skin (13, 14).

A strong correlation between the partition coefficients K describing the interaction of these compounds with DMPC preparations obtained from both the release and

the incorporation protocols used in the ITC experiments and the ER_J is observed, as seen in the histograms shown in Fig. 7. Similarly, there is a strong correlation between the crosspeak volume obtained from NOESY studies and the flux ER , as shown in Fig. 7. This correlation is to be expected if the crosspeak volume values primarily reflect the occupancy of the DMPC bilayer by the iminosulfuranes; note, however, the caveats mentioned in the NMR portion of the Results section. A similar correlation with the Q_{24} and the partition coefficients and crosspeak volumes has been observed, but is not illustrated graphically, because the ER_J and the Q_{24} do not vary independently of each other.

CONCLUSIONS

A number of correlations between the experimental physico-chemical results obtained for DMPC-iminosulfurane interactions and the skin penetration enhancement activities of iminosulfuranes have been noted. Iminosulfurane 3 stands out from other compounds of the series in respect to both its superior biological activity and its vastly different interaction with DMPC, including a possible enhanced residence time in the lipid bilayer suggested by ITC experiments. The results of this work strongly suggest that compound 3 facilitates the penetration of hydrocortisone, the model drug used, through the lipophilic regions of the skin. 

The Georgia Research Alliance provided funding for the purchase of the calorimeters and NMR spectrometer used in this

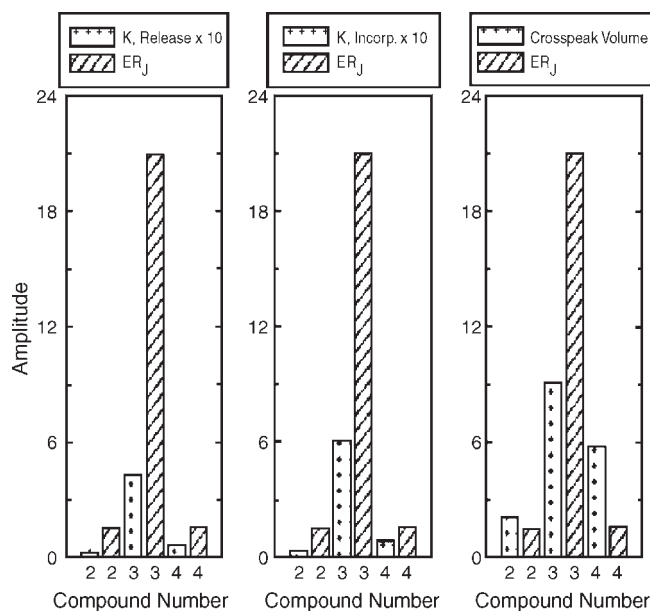


Fig. 7. The correlation between the partition coefficient K obtained from isothermal titration calorimetry measurements based on the release protocol (left panel), the partition coefficient K obtained via the incorporation protocol (middle panel), and the crosspeak volume obtained through NOESY spectroscopy (right panel) and the enhancement ratio ER_J observed in permeability studies using the three iminosulfuranes listed on the abscissa of the histograms.

TABLE 5. The entropy change associated with the partitioning of iminosulfuranes 2–4 into the DMPC bilayer and the experimentally determined parameters from which ΔS was determined

| Compound | K (1/mM) | ΔH (kJ/mol) | ΔS (J/K/mol) |
|----------|------------|---------------------|----------------------|
| 2 | 0.0275 | -26.55 | -116 |
| 3 | 0.429 | -2.590 | -15 |
| 4 | 0.0659 | -38.32 | -147 |

investigation. These investigations have benefited from the assistance of Professor David Hamilton with the calorimetry experiments and from the expert aid of Dr. Josef Salon and Mr. Randy Trammell with graphics.

REFERENCES

1. Hadgraft, J. 1999. Passive enhancement strategies in topical and transdermal drug delivery. *Int. J. Pharm.* **184**: 1–6.
2. Madison, K. C., D. C. Swartzendruber, P. W. Wertz, and D. T. Downing. 1987. Presence of intact intercellular lipid lamellae in the upper layers of the stratum corneum. *J. Invest. Dermatol.* **88**: 714–718.
3. Garson, J., J. Doucet, J. Leveque, and G. Tsoucaris. 1991. Oriented structure in human stratum corneum revealed by X-ray diffraction. *J. Invest. Dermatol.* **96**: 43–49.
4. Schurer, N. J., and G. Lee. 1992. The biochemistry and function of stratum corneum lipids. In *Advances in Lipid Research*, P. M. Elias, editor. Academic Press, New York.
5. Sekura, D. L., and J. Scala. 1988. The percutaneous adsorption of alkyl methyl sulfoxides. *Adv. Biol. Skin.* **12**: 257–269.
6. Hadgraft, J., J. Peck, D. G. Williams, W. J. Pugh, and G. Allan. 1996. Mechanisms of action of skin penetration enhancers/retarders: Azone® and analogues. *Int. J. Pharm.* **141**: 17–25.
7. Tsuzuki, N., O. Wong, and T. Higuchi. 1988. Effect of primary alcohols on percutaneous adsorption. *Int. J. Pharm.* **46**: 19–23.
8. Aungst, B. J., N. J. Rogers, and E. Shefter. 1986. Enhancement of naloxone penetration through human skin in vitro using fatty acids, fatty alcohols, surfactants, sulfoxides and amines. *Int. J. Pharm.* **33**: 225–234.
9. Bouwstra, J. A., M. A. Salomons-de Vries, B. A. I. van den Bergh, and G. S. Gooris. 1996. Changes in lipid organization of the skin barrier by N-alkyl-azocycloheptanones: a visualization and X-ray diffraction study. *Int. J. Pharm.* **144**: 81–89.
10. Bouwstra, J. A., G. S. Gooris, M. A. Salomons-de Vries, and W. Bras. 1992. The influence of N-alkyl-azones on the ordering of lamellae in human stratum corneum. *Int. J. Pharm.* **79**: 141–148.
11. Bouwstra, J., M. de Vries, G. Gooris, W. Bras, J. Brussee, and M. Ponc. 1991. Thermodynamic and structural aspects of the skin barrier. *J. Control. Release.* **15**: 209–219.
12. Harrison, J. E., P. W. Groundwater, K. R. Brain, and J. Hadgraft. 1996. Azone®-induced fluidity in human stratum corneum. A fourier transform infrared spectroscopy investigation using the perdeuterated analogue. *J. Control. Release.* **41**: 283–290.
13. Strekowski, L., M. Henary, N. Kim, and B. Michniak. 1999. N-(4-bromobenzoyl)-S,S-dimethyliminosulfurane, a potent dermal penetration enhancer. *Bioorg. Med. Chem. Lett.* **9**: 1033–1034.
14. Kim, N., M. El-Khalili, M. Henary, L. Strekowski, and B. Michniak. 1999. Percutaneous penetration enhancement activity of aromatic S,S-dimethyliminosulfuranes. *Int. J. Pharm.* **187**: 219–229.
15. Hu, B., F-Y. Sun, M-U. Long, and G-D. Huang. 2003. Study on synthesis and applications of laurocapram. *Chem. Abstr.* **32(5)**: 20–22.
16. Guo, J., C. Xie, and Y. Bao. 1999. Synthesis and applications of Azone. *Chem. Abstr.* **12**: 6–7.
17. Michniak, B. B., J. M. Chapman, and K. L. Seyda. 1993. Facilitated transport of two model steroids by esters and amides of clofibrac acid. *J. Pharm. Sci.* **82**: 214–219.
18. Song, Y. 2004. Investigation of Percutaneous Penetration: skin barrier function and its modulation, Ph.D. dissertation, Graduate School of Biomedical Sciences, University of Medicine and Dentistry of New Jersey, Newark, NJ.
19. Suurkuusk, J., B. Lentz, Y. Barenholtz, R. Biltonen, and T. A. Thompson. 1976. A calorimetric and fluorescent probe study of the gel-liquid crystal phase transition in small, single-lamellar dipalmitoylphosphatidylcholine vesicles. *Biochemistry.* **15**: 1393–1401.
20. Bammel, B., J. Brand, R. Simmons, and J. C. Smith. 1987. The interaction of potential-sensitive molecular probes with dimyristoylphosphatidylcholine vesicles investigated by ³¹P NMR and electron microscopy. *Biochim. Biophys. Acta.* **896**: 136–152.
21. Heerklotz, H., H. Binder, and R. Eppard. 1999. A “release” protocol for isothermal titration calorimetry. *Biophys. J.* **76**: 2606–2613.
22. Heerklotz, H., and J. Seelig. 2000. Titration calorimetry of surfactant-membrane partitioning and membrane solubilization. *Biochim. Biophys. Acta.* **1508**: 69–85.
23. Schirmer, N. 1971. The Nuclear Overhauser Effect: Chemical Applications. Academic Press, New York.
24. Gray, G. Magnetic Moments. *Varian Associates Newsletter.* **7**: 3033.
25. Brown, D. E. 1995. Fully automated base-line correction of 1D and 2D NMR-spectra using Bernstein polynomials. *J. Magnetic Res.* **A114**: 268–270.
26. Frisch, A., and M. Frisch. 1999. Gaussian 98 User’s Reference, 32, Gaussian Inc., Pittsburgh, PA.
27. van Duijnen, P., and M. Swart. 1998. Molecular and atomic polarizabilities: Thole’s model revisited. *J. Phys. Chem. A.* **102**: 2399–2407.
28. Biltonen, R. L., and E. Freire. 1978. Thermodynamic characterization of conformational states of biological macromolecules using differential scanning calorimetry. *CRC Crit. Rev. Biochem.* **5**: 85–124.
29. Thompson, L. K., J. M. Sturtevant, and G. W. Brudvig. 1986. Differential scanning calorimetric studies of photosystem II: evidence for a structural role for cytochrome b559 in the oxygen-evolving complex. *Biochemistry.* **25**: 6161–6169.
30. Zimm, B. H., and J. K. Bragg. 1959. Theory of the phase transition between helix and random coil in polypeptide chains. *J. Chem. Phys.* **31**: 526–535.
31. Rolland, A., A. Brzokewicz, B. Shroot, and J. Jamouille. 1991. Effect of penetration enhancers on the phase transition of multilamellar liposomes of dipalmitoylphosphatidyl choline. A study by differential scanning calorimetry. *Int. J. Pharm.* **76**: 217–224.
32. Rolland, A., A. Brzokewicz, B. Shroot, and J. Jamouille. 1990. A differential scanning calorimetric study of the effect of penetration enhancers on the thermal behavior of dipalmitoylphosphatidyl choline multilamellar vesicles. In *Prediction of Percutaneous Penetration*. R. Scott, R. Guy, J. Hadgraft, and H. Bodde, editors. IBC Technical Services, London. 110.
33. Salomons-de Vries, M., G. Gooris, C. Holl, M. Ponc, and J. Bouwstra. 1991. Proceedings and program of the 18th International Symposium on controlled release of bioactive materials: July 8–11, 1991, in Amsterdam, The Netherlands.
34. Huster, D., K. Arnold, and K. Gawrisch. 1999. Investigation of lipid organization in biological membranes by two-dimensional nuclear Overhauser enhancement spectroscopy. *J. Phys. Chem. B.* **103**: 243–251.
35. Gazzara, J. A., M. C. Phillips, S. Lund-Katz, M. N. Palgunachari, J. P. Segrest, G. M. Anantharamaiah, W. V. Rodriguez, and J. W. Snow. 1997. Effect of vesicle size on their interaction with class A amphipathic helical peptides. *J. Lipid Res.* **38**: 2147–2154.